THE JOURNAL OF PHYSICAL CHEMISTRY A

 VOLUME 110, NUMBER 17, MAY 4, 2006

ARTICLES

Effect of Electrolytes on the Excited-State Proton Transfer and Geminate Recombination

Pavel Leiderman, Rinat Gepshtein, Anna Uritski, Liat Genosar, and Dan Huppert*

Raymond and Beverly Sackler Faculty of Exact Sciences, School of Chemistry, Tel Aviv University, Tel Aviv 69978, Israel

Received: January 10, 2006; In Final Form: February 26, 2006

Time-resolved emission and steady-state fluorescence techniques are used to study the excited-state intermolecular proton transfer from 8-hydroxypyrene-1,3,6-trisulfonate (HPTS or pyranine) to water in the presence of inert salts, NaCl and $MgCl_2$. At low salt concentrations, up to about 0.5 M $MgCl_2$ or about 0.8 M NaCl, the time-resolved emission of both the photoacid and conjugate base can be quantitatively fitted by our diffusion-assisted geminate recombination model. In this concentration range, the proton transfer and geminate recombination rate constants are almost independent of the salt concentrations whereas the proton diffusion constant decreases as the salt concentration increases. At higher salt concentrations, the proton-transfer rate constant decreases while the recombination rate constant increases slightly. For the saturated solution of $MgCl_2$ (about 5 M at room temperature), the steady-state emission consists of only a single band of the protonated photoacid. Careful examination of the time-resolved emission of HPTS in the presence of a large concentration of $MgCl_2$ shows that the quality of the fit to the geminate recombination model is rather poor and we fail to find adjustable parameters for a good quality fitting. For this large concentration range of $MgCl_2$ we were able to get a good fit of the experimental data with a model based on a distribution of proton-transfer rates. The model is consistent with an inhomogeneous water environment next to the excited HPTS molecule in such concentrated solutions.

Introduction

Proton-transfer reactions are ubiquitous in chemical and biological processes.[1−4] Over the last two decades, intermolecular proton transfer in the excited state (ESPT) has been studied extensively both theoretically and experimentally and provided valuable information about the mechanism and nature of acid−base reactions.[5−12]

To initiate these reactions, protic solvent solutions of suitable organic molecules are irradiated by short (femtosecond-picosecond) laser pulses.[13−15] Consequently, the excited-state molecules dissociate very rapidly by transferring a proton to a nearby solvent molecule. 8-Hydroxypyrene-1,3,6-trisulfonate (HPTS or pyranine) is a photoacid commonly used in the study of the ESPT process.[15−17] The RO^- form is quadruply negatively charged. Thus, the reversible geminate recombination process is strongly enhanced relative to a singly charged photoacid like 2-naphthol. The proton-transfer rate could be determined by either the initial decay time of the time-resolved fluorescence of the protonated form (ROH) measured at 440 nm or the slow rise time of the emission of the deprotonated species (RO^-) at about 520 nm.

Over the past decade we used a model for an intermolecular ESPT process that accounts for the geminate recombination of the transferred proton. In this model, the overall dissociation process can be subdivided into the two consecutive steps of reaction and diffusion. In the reactive stage, a rapid short-range charge separation occurs and a solvent-stabilized ion pair is

* Corresponding author. E-mail: huppert@tulip.tau.ac.il. Phone: 972-3-640701. Fax: 972-3-6407491.

10.1021/jp060170j CCC: $33.50
Published on Web 04/01/2006

formed. This is followed by a diffusive stage, when the two ions withdraw from each other due to their thermal random motion. The reverse process is geminate recombination (neutralization) of the two separated ions either by the direct collapse of the ion pair or by following a geminate reencounter of the solvated "free" ions.

The effect of an inert salt ($NaNO_3$) at low concentrations on the time-resolved emission of the ROH band of HPTS was studied by Agmon et al.[18] The experimental results were quantitatively compared with the reversible geminate recombination model. We used the Debye−Hückel screened Coulomb potential to account for the salt screening effect. The proton-transfer rate and the geminate recombination rate were nearly independent of the salt concentration up to a concentration of about 160 mM.

Two decades ago we studied the rate of proton transfer from photoacids to the solvent in concentrated aqueous solutions (1−6 M) of strong electrolytes[19] (LiBr, $LiClO_4$, NaCl, NaClO, KCl, $MgCl_2$, $Mg(ClO_4)_2$. The rate of dissociation decreases upon increasing the concentration of the salt. Results obtained with different salts fit a single straight line when the log of the rate constant is drawn vs the log of water activity. It was proposed[19] that the rate of proton dissociation is related to the free energy of proton hydrate formation. Pines et al.[16] found, for a series of photoacids, a free energy relation between the logarithm of the proton-transfer rate constant and the free energy of the acid−base reaction in the excited state ΔG^*. A simple explanation of the large decrease in the proton-transfer rate in a large salt concentration solution is the ΔG increase of the reaction as a function of the salt concentration. The increase in ΔG may arise from the decrease of the proton hydrate complex number in the concentrated salt solution. The minimum number of hydration of ions, including that of the proton, was deduced by Hasted and co-workers[17] from the dielectric constant depression. The hydration number of Mg^{2+} , H^+ and Na^+ are 14, 10 and 4, respectively. Kebarle[20] measured the clustering of water molecules around free protons in the gas phase. They found that the hydration enthalpy increases with the increasing in the cluster number. Thus, we expect that small H^+ clusters are less stable and, as a consequence, the ΔG of the ESPT reaction in a small proton hydrate will increase and hence the rate constant of ESPT will be smaller. In a concentrated magnesium salt aqueous solution the fraction of free water versus the fraction of water bound to Mg^{2+} decreases as the salt concentration increases. The net result of a large concentration of Mg^{2+} is smaller H^+ water complexes.

In this study we follow our pioneering work of the salt effect on the ESPT process in aqueous concentrated salt solutions conducted more than two decades ago.[19] The new aspects of this work are the use of the reversible geminate recombination model for data analysis and the use of the time-correlated single photon counting technique to measure the time-resolved emission of both the ROH and RO^- bands. This experimental method provides excellent sensitivity, a large dynamic range and low intensity illumination conditions. The photoacid is HPTS and the salts are NaCl and $MgCl_2$. The Mg^{2+} ion has a small radius of 0.61 Å and thus has a profound effect on its close molecular environment.

In our previous study as well as this one, we found that the ESPT quantum yield drops from a value close to 1 in neat water to 0 for a saturated $MgCl_2$ aqueous solution (about 5 M at room temperature).[19] For a comparison with the strong effect of Mg^{2+} on ESPT we also measured the ESPT of HPTS in a NaCl solution, which exhibits a much milder effect even in 5.8 M solutions. The main finding of this study is that at high concentrations of $MgCl_2$, $c > 2$ M the time-resolved fluorescence decay of the photoacid, ROH, is nonexponential even at much shorter times than the inverse of the proton-transfer rate, $t < 1/k_d$, where k_d is the proton-transfer rate constant. Over this short time range the reversible geminate recombination model predicts a nearly exponential decay, especially when the Coulomb potential is almost totally screened by the salt ions.

We explained the surprising experimental findings by the proton-transfer rate in a concentrated salt solution not having a single value (exponential decay) but rather a distribution of rates arising from the distribution of the microenvironment next to the HPTS and hence the measured proton-transfer rate is nonexponential.

Experimental Section

Time-resolved fluorescence was acquired using the time-correlated single-photon counting (TCSPC) technique, the method of choice when sensitivity, large dynamic range and low intensity illumination are important criteria in fluorescence decay measurements.

For excitation, we used a cavity dumped Ti:sapphire femtosecond laser, Mira, Coherent, which provides short, 80 fs, pulses of variable repetition rate, operating at the SHG frequency, over the spectral range of 380−400 nm with the relatively low repetition rate of 500 kHz. The TCSPC detection system is based on a Hamamatsu 3809U, photomultiplier and Edinburgh Instruments TCC 900 computer module for TCSPC. The overall instrumental response was about 35 ps (fwhm). Measurements were taken at 10 nm spectral width. The excitation pulse energy was reduced by neutral density filters to about 10 pJ. We checked the sample's absorption prior to and after time-resolved measurements. We could not find noticeable changes in the absorption spectra due to sample irradiation.

Steady-state fluorescence spectra were taken using a FluoroMax (Jobin Yvon) spectrofluorimeter. The HPTS, of laser grade was purchased from Kodak or Aldrich. $MgCl_2$ and NaCl (analytical grade) were purchased from Aldrich. Perchloric acid, 70% reagent grade was purchased from Aldrich. For steady-state fluorescence measurements we used solutions of $\sim 2 \times 10^{-5}$ M of HPTS.

Reversible Diffusion-Influenced Two Step Proton-Transfer Model. The model is based on a Smoluchowski-level approach for the relative diffusive motion of the geminate proton−anion pair.[17] The separated pair at time t, $p(r,t)$ is assumed to obey a spherically symmetric Debye−Smoluchowski equation (DSE) in three dimensions, which is coupled to a kinetic equation for the ROH probability, $P(t)$

$$\frac{\partial p(r,t)}{\partial t} = \left[r^{-2}\frac{\partial}{\partial r}Dr^2 e^{-V(r)}\frac{\partial}{\partial r}e^{V(r)} - k_0'\right]p(r,t) + [k_{PT}P(t) - k_a p(r,t)]\frac{\delta(r-a)}{4\pi a^2} \quad (1a)$$

$$\frac{\partial}{\partial t}P(t) = k_{PT}p(a,t) - (k_d + k_0)P(t) \quad (1b)$$

The geminate recombination is given by a delta function "sink term", $k_a\delta(r-a)/(4\pi a^2)$. In contrast, the ROH* and RO^-* radiative decay constants (k_0 and k_0', respectively) are r-independent. The mutual attraction of the proton and the HPTS anion is described by a distance-dependent potential, $V(r)$, in units of the thermal energy k_BT. In this study the ESPT process is examined in the presence of large salt concentration in

aqueous solution. We therefore apply the screened Coulomb potential of Debye and Hickel[21]

$$V(r) = -\frac{R_D}{r}\frac{\exp[-\kappa_{DH}(r-a)]}{1+\kappa_{DH}a} \quad (2)$$

where R_D and κ_{DH}^{-1} are the Debye and ionic-atmosphere radii, respectively, and a is its ionic radius.

$$R_D \equiv \frac{|z_1 z_2|e^2}{\epsilon k_B T}$$

$$\kappa_{DH}^{\ 2} \equiv \frac{8\pi e^2 c}{\epsilon k_B T}$$

$$\kappa_{DH} \equiv A\sqrt{c} \quad (3)$$

$z_1 = 1$ and $z_2 = -4$ are the charges of the proton and deprotonated HPTS, respectively, e is the electronic charge, ϵ is the static dielectric constant of the solvent, k_B is Boltzmann's constant, T is the absolute temperature and c is the concentration of the electrolyte.

The relative diffusion constant, D, is the sum of the protic and anionic diffusion coefficients. Because the proton is abnormally fast, whereas the anion is bulky and slow, its diffusion coefficient may be neglected with respect to that of the proton. We do not employ any distance dependence in D, mainly because procedures for doing so are not well-established.

As compared with traditional treatments of diffusion-influenced reactions,[22] the new aspect is the reversibility of the reaction, described by the "back-reaction" boundary condition.[17,23,24]

The process we wish to consider begins upon photochemical excitation, which prepares a thermally and vibrationally equilibrated ROH* acidic form in the lowest electronic state, S_1. Thus, the initial condition is

$$p(*,0) = 1 \qquad p(r,0) = 0 \quad (4)$$

Subsequently, the bound and dissociated states evolve according to eq 1. We solve these equations numerically using the for solving the spherically symmetric diffusion problem (SSDP) Windows application,[25] convolute $p(*,t)$ with the IRF and compare it with the ROH* fluorescence signal.

The asymptotic expression (the long-time behavior) for the fluorescence of ROH* is given by[24]

$$[\mathrm{ROH}^*]\exp[t/\tau_f] \cong \frac{\pi}{2}a^2(\exp[V(a)])\frac{k_r}{k_d(\pi D)^{3/2}}t^{-d/2} \quad (5)$$

where τ_f is the excited-state lifetime of the deprotonated form RO^-, d is the dimensionality of the relevant problem, a is the contact radius and k_d and k_r are the proton transfer and recombination rate constants, respectively. All other symbols are as previously defined. Equation 5 shows that the tail amplitude depends on several parameters but its time dependence is a power law of time that depends on the dimensionality of the problem. For 3 dimensions it assumes the power law of $t^{-3/2}$.

k_d determines the initial slope of the decay curves: the larger k_d, the faster the initial exponential drop. The intrinsic recombination rate constant, k_r, does not affect the behavior at $t \to 0$ but determines the magnitude of the long-time tail. The effect of increasing k_r is somewhat similar to decreasing D. It differs from the effect of changing R_D or a in the curvature of these plots. The parameters for the numerical solution of the DSE were taken from the literature.[21,26] The contact radius $a = 6$ Å is slightly larger than the molecule's spherical gyration radius (4.5−5.5 Å) obtained from measurements of HPTS rotation times.[27] It probably accounts for at least one layer of water molecule around the HPTS anion.

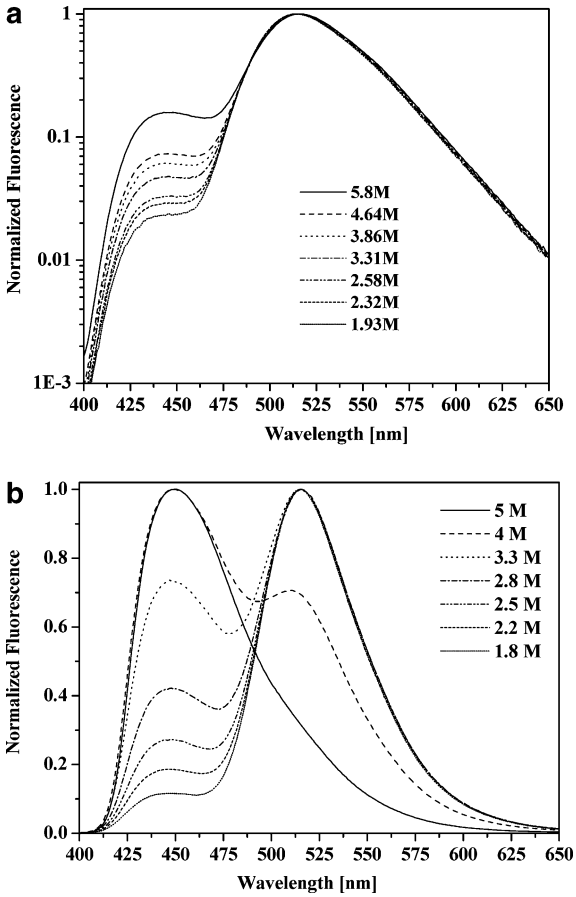

Figure 1. Steady-state emission spectra of HPTS in various concentrations of inert salts: (a) NaCl; (b) $MgCl_2$.

The absolute fluorescence quantum yield of ROH is given by

$$\Phi(\mathrm{ROH}^*) = \tau_f^{-1}\int_0^\infty P(t)\exp(-t/\tau_f)\,dt \quad (6)$$

P(t) is given by

$$P(t) = 1 - Q(t) \quad (7)$$

$$Q(t) = 4\pi\int_a^\infty p(r,t)\,dr \quad (8)$$

Results

Parts a and b of Figure 1 show the steady-state emission of HPTS in water NaCl and $MgCl_2$ solutions, respectively. For large salt concentrations, $c \geq 0.5$ M, the intensity of the ROH emission band at 440 nm increases as the salt concentration increases. For $MgCl_2$ at concentrations higher than $c \geq 3.2$ M, the ROH band intensity at 440 nm is larger than the intensity of the RO^- band whose peak position is at 510 nm.

The radiative rates of both ROH and RO^- are about the same, $\tau \geq 5.4$ ns, and almost independent of the salt concentration. We attribute the changes in the relative emission intensity of the ROH and RO^- bands of the steady-state spectra with salt concentration to the large changes in the proton-transfer rates at large salt concentrations especially in the case of the

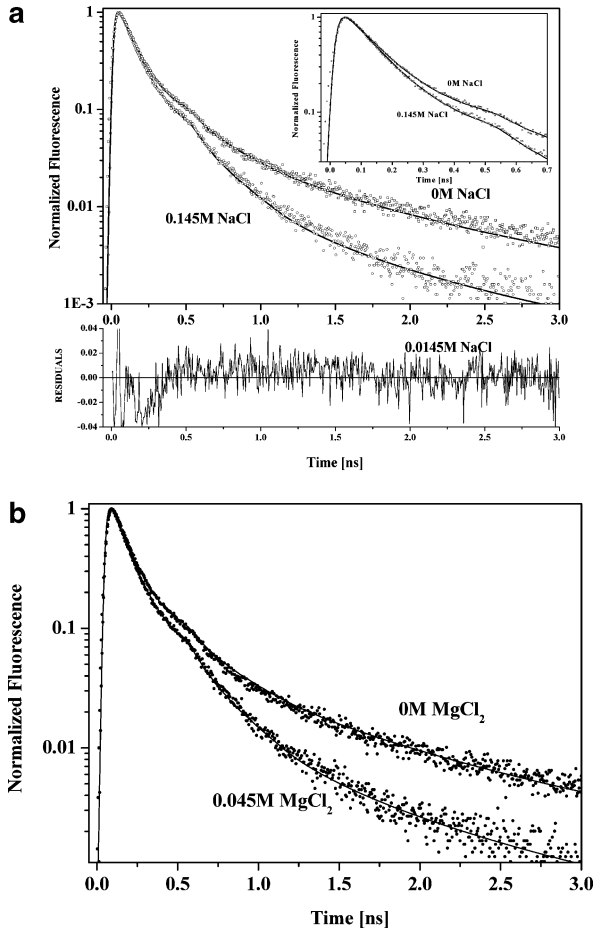

Figure 2. (a) Semi-log plot of the time-resolved emission and the computer fit using the geminate recombination model of the ROH band of HPTS in water and in a 0.145 M NaCl solution. (b) As for (a) but the salt solution contains 0.045 M $MgCl_2$.

$MgCl_2$ solution. When $k_d < k_{rad}$, where k_{rad} is the radiative rate constant ($k_{rad} = 1/\tau$), the ESPT quantum yield drops sharply and the fluorescence intensity of RO^- diminishes drastically.

Figure 2 shows on a semi-log plot the time-resolved emission of the ROH band of HPTS in neat water and 60 mM NaCl and similar results for the $MgCl_2$ solution. The fluorescence tail arises from the geminate recombination model. For low salt solutions, $c \leq 0.2$ M, the intensity of the long-time fluorescence tail decreases sharply because the Coulomb attraction between RO^- and the proton is screened by the salt ions, whereas the proton-transfer rate is not affected by the presence of the salt.

Parts a and b of Figure 3 show on 10 and 3 ns time scales, respectively, the time-resolved emission of the protonated form measured at 435 nm in the NaCl solutions. The signal of the RO^- of HPTS in aqueous solutions of various NaCl salt concentrations measured at 515 nm is shown in Figure 3c. For high salt concentration, the short time decay rates of the ROH band decreases as the salt concentration increases. The short time decay of the ROH band is attributed to the ESPT process, and thus the proton-transfer rate decreases as the salt concentration increases. The solid line in the figure is a computer fit to the proton-transfer geminate recombination model.

Parts a and b of Figure 4 show on a semi-log plot the time-resolved emission of the ROH of HPTS in low and high concentrations, respectively, of $MgCl_2$ solutions along with the computer fit to the reversible geminate recombination model. As seen in the figure, the fit is rather good at concentrations up to about 2 M. We fit both the ROH and RO^- with the same

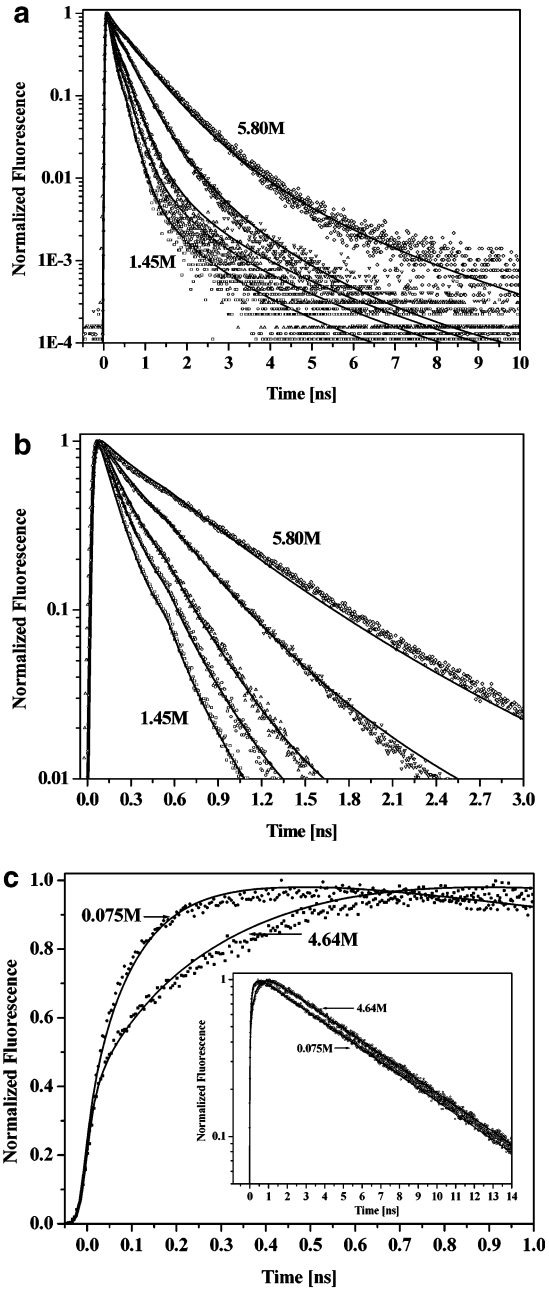

Figure 3. Time-resolved emission of HPTS in NaCl solutions: (circles) experimental results; (solid line) the computer fit to the geminate recombination model. (a) ROH signal on a 10 ns time scale measured for 435 nm at a concentrations of 1.45, 2.58, 3.31, 4.64 and 5.80 M. (b) Stretched time scale of 3 ns. (c) RO^- signal measured at 515 nm.

parameters. At higher concentrations, the quality of the computer fit is rather poor for short times. Figure 4c shows the ROH decay on a stretched time scale-up to 5 ns to emphasize the mismatch between the experimental data and the fit. In the discussion section, we suggest a plausible reason for the mismatch between the geminate recombination model and the experimental results. Figure 4d shows the time-resolved emission of the RO^- band of HPTS in neat water and in a 1.66 M $MgCl_2$ solution. As seen in Figure 4b,d, the decay of the ROH and the rise time of RO^- forms at 1.66 M are much slower than those in pure water because the proton-transfer rate in a high $MgCl_2$ salt concentration is much smaller than that in pure water. At 5 M the ESPT rate is slower than the radiative rate and thus the excited-state population mainly decays by the radiative process. It implies that the RO^- band intensity shown in the steady-state spectra

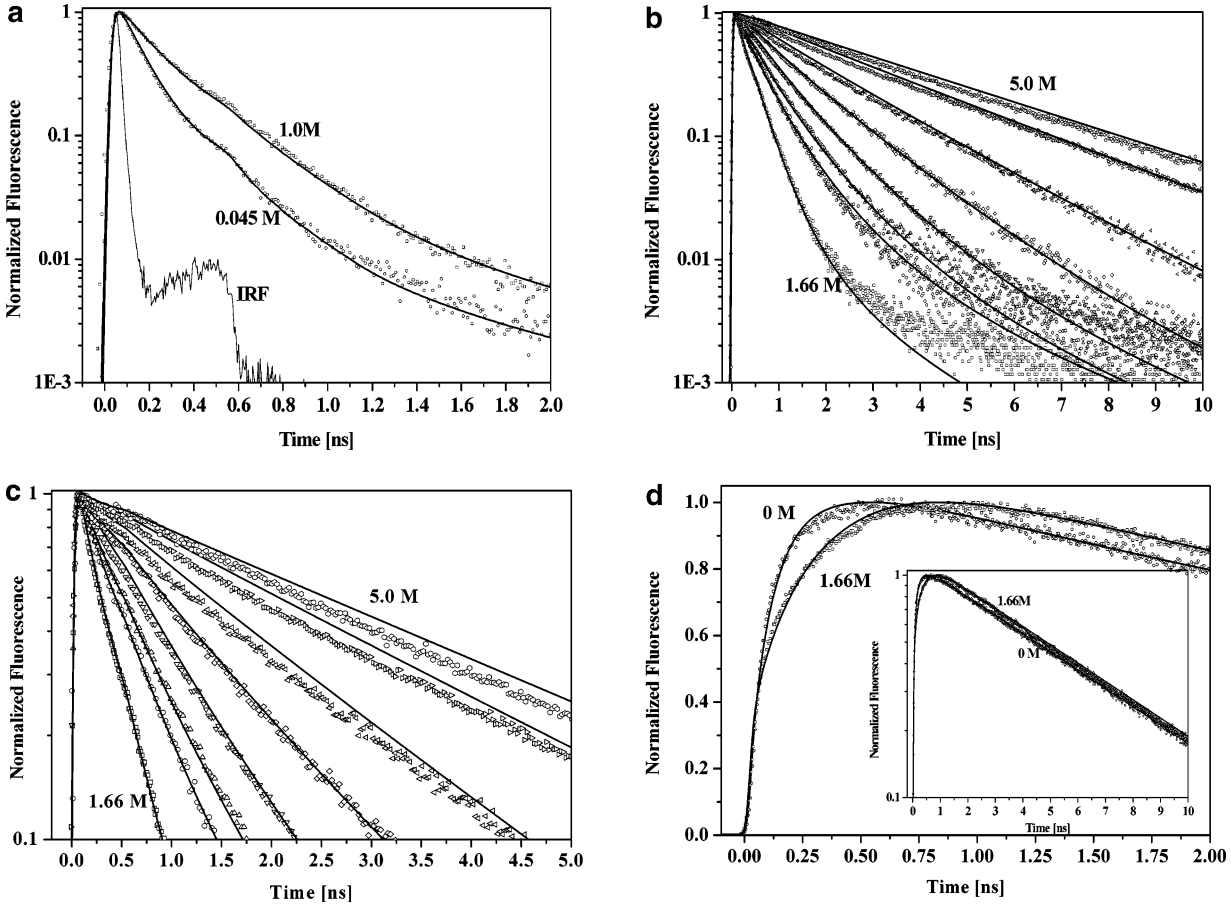

Figure 4. Time-resolved emission of HPTS in $MgCl_2$ solutions: (circles) experimental results; (solid line) the computer fit to the geminate recombination model. (a) ROH signal. (b) ROH signal of high salt concentrations, 1.66, 2.07, 2.50, 2.85, 3.26, 3.80 4.56 and 5.0 M. (c) ROH decay on a stretched time scale, up to 5 ns, to emphasize the mismatch between the experimental data and the fit. The RO^- signal in neat water and in a 1.66 M $MgCl_2$ solution.

in Figure 1b is smaller than the ROH band. In an $MgCl_2$ solution, the decrease in the ESPT rate constant is dramatic. At about 5 M $MgCl_2$, the rate decreases by a factor of 100.

The next subsection is devoted to the fine details of the fitting procedure and the salt concentration dependence of the parameters of the geminate recombination model. The fitting parameters are the diffusion constant D, the screened potential $V(r)$, the proton rate constant k_d and the recombination rate constant k_r. For high salt concentrations, k_d, k_r, the screened potential, $V(r)$, and D change with concentration and thus we have a multiparameter fitting problem.

Fitting Procedure Using the Geminate Recombination Model. In fitting the time-resolved data shown in Figures 2−4 (solid lines are the fitting curves), we used our model of proton transfer followed by reversible geminate recombination. The main consequence of the geminate recombination process is the repopulation of the ROH* form in the excited state, thus creating a nonexponential decay of the fluorescence. To quantitatively fit the experimental data, we need to know the dependence of the proton diffusion constant D_{H^+} in the presence of the salt and for the calculation of the screened Coulomb potential the dielectric constant as a function of the salt concentration. In water with low salt concentrations the excited-state lifetimes of the ROH and RO^- of HPTS are about the same, $\tau_f = 5.4$ ns. We found that, at high concentrations of $MgCl_2$, the excited-state lifetimes of both ROH and RO^- decrease somewhat. At about 5 M $MgCl_2$ the excited-state lifetimes of ROH and RO^- are about 4.5 ns.

The tracer diffusion of H^+ in the presence of alkali chloride salts is given in Table 11.7 of ref 21. It was found that the diffusion constant of H^+ decreases as the salt concentration increases. In NaCl, the relative proton diffusion constant (with respect to a salt-free solution) values are 0.87, 0.80 0.74 and 0.42 for solutions of 0.1, 0.5, 1 and 4 M NaCl. In a previous study[24] on time-resolved emission of HPTS in the presence of $NaNO_3$ we found that the decrease in the proton diffusion is larger by a factor of about 2 than previously reported in the literature. We are unaware of published results of the tracer diffusion of H^+ in the presence of $MgCl_2$. The effect of LiCl on the tracer diffusion of H^+ is much larger than that of NaCl. At 4 M LiCl, the relative diffusion constant is only 0.28.[21] Because $MgCl_2$ affects the properties of water more than LiCl, we assume that the reduction of the diffusion constant of H^+ is larger in $MgCl_2$ than in LiCl and NaCl. In the fitting of the time-resolved data we used a value for about $D = 10^{-5}$ cm^2/s at about 2.8 M $MgCl_2$.

For the calculations of the proton geminate recombination probability using the DSE (see eq 1) and the attraction potential between the RO^- of HPTS (eqs 2−3) we assume that the dielectric constant of water is about 78 for low and medium salt concentrations. At high salt concentrations, the use of the Debye−Hückel screening formula (see eq 3) probably does not hold and the screened Coulomb potential calculations are probably incorrect. Calculations using eq 3 show that in solutions of high salt concentrations with $c > 1$ M, the Coulomb potential at distances larger than $a = 6$ Å (the contact sphere radius in our model) is totally screened and approaches zero.

TABLE 1: Kinetic Parameters for the Proton-Transfer Reaction of HPTS in a H_2O/NaCl Solution Using the Reversible Geminate Recombination Model[a]

$C(Na^+)$, [M]	k_d [10^9 s^{-1}][b,c]	k_r [10^9 Å s^{-1}][b,d]	D [cm^2 s^{-1}][e]
0	9.0	5.5	1.0×10^{-4}
0.075	9.6	7.0	8.0×10^{-5}
0.145	9.6	7.2	7.0×10^{-5}
0.290	9.3	7.3	6.0×10^{-5}
0.580	9.6	7.5	5.0×10^{-5}
0.970	8.7	7.5	4.0×10^{-5}
1.45	7.7	7.5	3.5×10^{-5}
1.93	7.2	7.5	3.0×10^{-5}
2.32	6.9	7.5	2.8×10^{-5}
2.58	6.5	8.0	2.7×10^{-5}
3.31	5.2	8.0	2.4×10^{-5}
4.64	3.8	9.0	2.0×10^{-5}
5.80	2.5	19	1.7×10^{-5}

[a] There are some constant values: $R_D = 28$ Å, $\tau^{-1}_{ROH} = 0.18$ ns^{-1} and $\tau^{-1}_{RO-} = 0.19$ ns^{-1}. [b] k_d and k_r are obtained from the fit of the experimental data by the reversible proton-transfer model (see text). [c] The error in the determination of k_d and k_r at low salt concentration is 10% and 50%, respectively; see text. [d] The error in the determination of k_d at a large concentration of $MgCl_2$, $c > 2.3$ M, is 50%; see text. [e] Values at high concentrations obtained by best fit to the fluorescence decay.

TABLE 2: Kinetic Parameters for the Proton-Transfer Reaction of HPTS in a $H_2O/MgCl_2$ Solution Using the Reversible Geminate Recombination Model[a]

$C(Mg^{2+})$, [M]	k_d [10^9 s^{-1}][b,c]	k_r [10^9 Å s^{-1}][b,d]	D [cm^2 s^{-1}][e]
0	9.0	5.5	1.0×10^{-4}
0.045	9.3	6.5	8.0×10^{-5}
0.112	9.3	6.7	7.0×10^{-5}
0.225	9.3	7.0	5.0×10^{-5}
0.450	8.8	7.5	3.5×10^{-5}
0.833	6.2	7.5	2.8×10^{-5}
1.00	5.6	7.5	2.3×10^{-5}
1.66	4.0	8.0	2.0×10^{-5}
2.00	3.0	18	1.7×10^{-5}
2.20	2.4	16	1.5×10^{-5}
2.50	1.7	13	1.3×10^{-5}
2.86	0.90	8.0	1.2×10^{-5}
3.33	0.50	7.0	1.0×10^{-5}
4.00	0.230	5.0	7.0×10^{-6}
5.00	0.070	5.0	5.0×10^{-6}

[a] There are some constant values: $R_D = 28$ Å, $\tau^{-1}_{ROH} = 0.18$ ns^{-1} and $\tau^{-1}_{RO-} = 0.19$ ns^{-1}. [b] k_d and k_r are obtained from the fit of the experimental data by the reversible proton-transfer model (see text). [c] The error in the determination of k_d and k_r at low salt concentration is 10% and 50%, respectively; see text. [d] The error in the determination of k_d at a large concentration of $MgCl_2$, $c > 2.3$ M, is 50%; see text. [e] Values at high concentrations obtained by best fit to the fluorescence decay.

The fitting of the time-resolved emission of the ROH and RO^- bands of HPTS using the DSE model is shown in Figures 2−4 for both NaCl and $MgCl_2$, respectively. The fitting parameters are given in Tables 1 and 2. For the NaCl solution, the proton-transfer rate constant is almost constant up to 1 M concentration. At about 3.3 M, the rate constant decreases by a factor of 2. The geminate recombination rate constant is almost independent of the salt concentration up to 1 M. At higher concentrations, k_d decreases while k_r increases slightly with the increase of the salt concentration. The diffusion constant of H^+ decreases by a factor of 5 when the NaCl concentration is about 4.64 M.

The fit of the time-resolved emission in the presence of magnesium salt is more complicated because the changes in the fitting parameters k_d, k_r and D are much larger. The proton-transfer rate constant, k_d, decreases by a factor of about 100 at 5 M $MgCl_2$ (saturated solution at room temperature). The recombination rate constant increases slightly with salt concentration up 2.5 M. At concentrations above 2.8 M, k_r decreases with salt concentration. At those high concentration ranges the proton-transfer rate constant k_d is small and thus it is difficult to differentiate between k_d (the short times) and k_r (the intermediate time). The proton diffusion constant decreases by about an order of magnitude. The overall effect of the large reduction in k_d and D is that the HPTS steady-state emission spectrum of a saturated $MgCl_2$ solution of pH ≈ 6 (pK ∼ 7.7) excited at the ROH band consists of only the emission band of the protonated form.

The asymptotic expression for the long-time fluorescence tail of the ROH form is given by eq 5. The parameters that control the relative amplitude of the tail are $e^{V(a)}$, k_d, k_r and D. All these parameters are strongly affected by the $MgCl_2$ concentration. As a consequence of the salt concentration increase ($c \geq 1$ M), the amplitude of the ROH fluorescence tail increases. At about 5 M $MgCl_2$ the relative change of the parameters with respect to neat water values are $D(5\text{ M})/D^0 = 0.1$, $k_d(5\text{ M})/k_d^0 = 0.01$ and $k_r(5\text{ M})/k_r^0 = 3$. Assuming that at 5 M $e^{V(a)} = 1$, then $e^{V(a)}$-$(5\text{ M})/e^{V(a)} = 0.02$.

Calculating the tail amplitude in neat water and in 5 M $MgCl_2$ using eq 5 shows that the long-time fluorescence amplitude of HPTS in 5 M $MgCl_2$ increases by a factor of about 400 with respect to neat water. These large changes drastically affect the fitting capability and the uniqueness of the values of the parameters used to fit the shape of the time-resolved emission of both ROH and RO^- of HPTS in a concentrated solution of $MgCl_2$.

In fitting the time-resolved emission of HPTS in neat water the only adjustable parameters are k_d and k_r. k_d mainly affects the time-resolved signal at short times (head) whereas k_r affects the longer times, i.e., the fluorescence shape at intermediate times and the height of the long-time fluorescence tail. In neat water the fluorescence decay for short times is fast and nearly exponential. The long-time nonexponential tail is well separated from the initial decay. In neat water, the contribution of the geminate recombination k_r to the early times is relatively small whereas that of k_d is large. At low salt concentrations, the main effect on the luminescence of ROH is the strong decrease in the amplitude of the long-time fluorescence tail. This is due to the Coulomb potential screening by the salt ions. In contrast to the neat water and the low salt concentration, in fitting the high salt concentrations (of about $c > 1.5$ M of $MgCl_2$) we find that the contribution of the recombination process to the early times is larger than that in water. The amplitude of the long-tail (given in eq 5) is determined by the ratio $k_r/(k_d D^{3/2})$. It is much larger than that in neat water. Because k_d drastically decreases with salt concentration, the separation between the contribution of k_d and k_r for long times is unclear. One can get a similar fitting of the ROH and RO^- curves with a relatively small k_d and small k_r and vice versa. We find that at high $MgCl_2$ concentrations ($c > 2.5$ M), the ROH decay is nonexponential even at early times (shorter than 2 ns) where k_d is relatively small ($k_d < 0.5$ ns^{-1}) and comparable with the radiative rate $k_{rad} = 0.2$ ns^{-1}. In these high salt concentrations, we find (see Figure 4) that the geminate recombination model fails to quantitatively fit the ROH decay for all combinations of reasonable k_d, k_r and D values. The mismatch between the model and the experimental results leads us to propose a specific model for high concentration salt solutions. To achieve better results when fitting the ROH time-resolved emission experimental results for high salt concentrations, we developed a simple model based on the hypothesis

that, at a high Mg^{2+} concentrations, the solution next to the hydroxyl group is not homogeneous but rather an inhomogeneous environment. In the discussion section we describe the inhomogeneous water cluster model.

Discussion

In a previous study[19] published more than two decades ago about the rate of proton transfer of photoacids in aqueous solutions, in the presence of a large concentration of various electrolytes we found that the rate measured in equimolar concentrations of NaCl, LiBr, or $MgC1_2$ varied markedly. The activity of H_2O that reflects the properties of the solvent in the solution, was found suitable to describe the change in the proton-transfer rate with the concentration of the various salts. Experimental results obtained with the three electrolytes fit a single linear function

$$\log k_d = \log k_d^0 - n \log a(H_2O) \tag{9}$$

where k_d and k_d^0 are the proton-transfer rate in salt solutions and pure water, respectively. Equation 9 is compatible with a reaction mechanism where the excited molecule transfers a proton to a hydration complex of n water molecules. The plot of the logarithm of the proton-transfer rate constant of HPTS versus the log of water activity gave a slope of about 7. Such a presentation is a gross oversimplification as n becomes a stoichiometic factor stating that no reaction will take place with the species $(H_2O)_{n-1}$ or $(H_2O)_{n+1}$. Thus, a less stringent explanation should be sought. In this study, we use the guidelines of the previous study and extend the proton hydration cluster model. The main experimental finding in the current study is the nonexponential decay of the time-resolved emission of the ROH in concentrated $MgCl_2$ solutions even at short times $t < 1/k_d$, where k_d is the proton-transfer rate constant. To explain this unexpected finding, we invoke that in concentrated $MgCl_2$ solutions the close region of water molecules surrounding the HPTS molecule forms an inhomogeneous environment. The measured nonexponential decay rate of proton-transfer arises from an excited ensemble of photoacids with a distribution of rates due to the inhomogeneous environment.

Searcy and Fenn[28] and Kebarle[20] measured the clustering of water molecules around free protons in the gas phase. Clusters of various sizes were observed and the respective enthalpy of formation was calculated. The difference in enthalpy of the hydration of a proton vs the cluster number n, designated as $-\Delta H^0_{n,n+1}$, shows a remarkable decrease with an increasing cluster number n. The hydration enthalpy difference between a monomer H_3O^+ and a dimer is $-\Delta H^0_{1,2} = 32$ kcal/mol and $-\Delta H^0_{2,3} = 22$ kcal/mol. These values are comparable with the results obtained from quantum-mechanical calculation.[29,30] The hydration enthalpy $-\Delta H^0_{n,n+1}$ reaches a limiting value of about 10 kcal/mol when the cluster number is about 10. By analogy with these results, the enthalpy of proton hydration in solution will also increase with the size of the hydration complex. Yet, in liquid water, one exception should be made: To increase the size of the complex by one water molecule, a water molecule must first be removed from the bulk, with an energy investment of 10 kcal/mol (heat of evaporation of water). Therefore, the hydration complex of a proton will not exceed the state where the energy gain of further hydration will be comparable with the heat of evaporation. Using the results of Kebarle[20] and Searcy and Fenn,[28] we estimate that the hydrating complex in a dilute electrolyte solution ($a_{H_2O} = 1$) will be of about 10 water molecules.

In concentrated salt solutions, the vapor pressure is lower than that of pure water and hence it exhibits reduced water activity. This phenomenon is explained by the fact that a considerable fraction of the water molecules are associated with the hydration of the salt ions. The binding energy of these water molecules (which form the first and second hydration shells), to the center ion, is larger than 10 kcal/mol. Therefore, they are less likely than the free water molecules to participate in the process of the hydration of the initially formed H_3O^+. To obtain a proton hydrate greater than H_3O^+, the thermodynamically stable complex must be formed within the ion-pair lifetime. The depletion from the solution of water molecules available for this reaction will lower the probability of the successful protolytic dissociation. As demonstrated in Figure 5 of ref 19, this function indeed decreases with the activity of the water in the solution.

From mobility measurements, vapor pressure depression and dielectric constant depression the effective number of bound water molecules around ions can be estimated.

The dielectric constant of a salt solution was studied by Hasted and co-workers.[31] They found that the dielectric constant decreases as the salt concentration increases. They found that the dielectric constant ϵ can be represented by a formula:

$$\epsilon \leq \epsilon_W + 2\,\bar{\delta} c \tag{10}$$

where ϵ_W is the dielectric constant of water, c is the concentration in molar units and $\bar{\delta}$ has a value between -5 and -15 for various salts in concentrations of up to 2 M.

According to Hasted,[31] it is possible to estimate the minimum hydration number of a cation from the value of δ^+ on the following basis: the model in which short range order dominates the orientation of the inner hydrogen sheath, effectively removing a fraction of water molecules from playing any part in the dielectric process; outside this there is a region in which a small amount of saturation takes place, so that these molecules make a small contribution to the fall of the dielectric constant. According to Hasted and co-workers it is reasonable to assume that this accounts for about a quarter of $\delta^+_{Na^+}$, that is, -2. Subtracting this contribution, they found in the inner sheath, N, for the minimum number of water molecules.

$$(-\delta^+ - 2)/\epsilon_W = NM/1000 \tag{11}$$

where M is the molecular weight of water.

Using eq 11 gives the minimum hydration of Na^+ and Mg^{2+} as about 4 and 14 water molecules, respectively. The above-mentioned theory connects the depression of the dielectric constant with the dielectric saturation of a definite number of water molecules in the first and second solvation layers around the cations for which the effective dielectric constant is $\epsilon \leq 4$. The dielectric constant of the rest of the water molecules assume the high value of water, i.e., $\epsilon = 78$. In 1 M $MgCl_2$ salt, basically 3/8 of the water molecules are bound as ion solvent molecules in solvation shells and only 5/8 of the water molecules have a regular large dielectric constant of 78.

The minimum hydration number of H^+ from Hasted and co-workers measurements[31] is 10. As mentioned above, this number can also be deduced from the enthalpy of formation of $H^+(H_2O)_n$ determined by Kebarle for gas-phase H^+ water clusters[19] The proton-transfer rate will be strongly dependent on the average proton hydrate size. It was previously found that the rate of proton-transfer correlates with the free energy of reaction, pK*. The lower the pK*, the faster the proton-transfer rate.[32] For high salt concentrations, the free water is situated in a small

space between the Mg^{2+} ions. It probably tends to organize as water clusters. For a 1 M salt concentration, the average distance between cations is 9.4 Å and for 5 M of salt the average distance is 5.5 Å. If the radius of a water molecule is approximately 1.6 Å and in $MgCl_2$ about two solvation layers are dielectrically saturated by the Mg^{2+} ion, then the average amount of free water surrounding the HPTS molecules will be less than 10.

The rate of exchange in water molecules of the first coordination sphere for several cations was studied by Eigen and Tamm[33] using ultrasonic absorption technique. It was found that the rate constant for water substitution around Mg^{2+} is very small, about 10^5 s^{-1}, whereas for the alkali cations the rate constant is much larger, in the range of 10^9 s^{-1}. When the water exchange rate is much slower than the proton-transfer rate constant and the free water is only a small fraction of the total water molecules (at large $MgCl_2$ concentrations), it is reasonable to use an inhomogeneous kinetics model that is based on the assumption that the number of free water molecules surrounding the HPTS is semi-fixed during the proton-transfer process. As mentioned above, the number of water molecules bound to a proton in low concentration acid solution is large and the average number of bound water molecules is about 10.

The main assumption in an inhomogeneous model described in the text section is that the rate of the proton transfer strongly depends on the water proton cluster size. Knochenmuss and co-workers[34] measured the excited-state proton-transfer rate of a 1-naphthol water cluster in the gas phase. They found that the proton-transfer rate depends on the average cluster size. For small clusters ($n < 100$), the average rate was slower by about a factor of 10 than the rate for larger clusters ($40 < n < 800$). The kinetics was multiexponential with picoseconds and nanoseconds components due to the large width of the distribution in the cluster size. The Knochenmuss and co-workers study clearly shows that the proton-transfer rate strongly depends on the water cluster size.

To obtain better results when fitting the ROH time-resolved emission experimental results at high salt concentrations, we developed a simple model based on the hypothesis that, at a high Mg^{2+} concentrations, the solution next to the hydroxyl group is not a homogeneous aqueous solution but rather an inhomogeneous microenvironment. The proton-transfer rate in solution depends also on the water cluster size $H_3O^+(H_2O)_n$.

Water Cluster Model. In the cluster model we assume that the rate of proton transfer strongly depends on the number of free water molecules surrounding the hydroxyl group of the HPTS. For high salt concentrations ($c \geq 0.5$ $MgCl_2$) the ratio between free and bound water ($[H_2O]_{free}/[H_2O]_{bound}$) decreases as the salt concentration increases. The average size of the free water cluster strongly depends on the salt concentration. The mathematical derivation is similar of that of ref 35, which deals with the radiationless transition of the GFP chromophore in solution.

In the proposed model, we assume that the proton is transferred to a water cluster of size n next to the hydroxyl group of HPTS. In salt solutions the water cluster size decreases as the salt concentration increases. The clusters form a distribution of its size. For simplicity we assume that the cluster distribution is Gaussian with a certain width defined by a variance σ and an average size $\bar{n}$. We will use a continuous coordinate x ($x \geq 0$) that is inversely related to the water cluster size n. The cluster distribution is given by

$$p(x) = \frac{1}{\sqrt{2\pi\sigma^2}} \exp\left[-\frac{(x - x_0)^2}{2\sigma^2}\right] \tag{12}$$

where x_0 is the mean (the peak position) of the Gaussian and is related to the average cluster size. We assume that the rate constant of proton transfer depends exponentially on the coordinate x, which is inversely related to the cluster size. At $x = 0.4$, the rate constant assumes the value of a neat water solution (for HPTS $k_d \sim 10$ ns^{-1}). The larger the value of x, the smaller the average cluster size. The rate constant is given by

$$k(x) = A \exp[-x] \tag{13}$$

In the static limit where the size of the cluster next to the hydroxyl group of HPTS is time-independent with respect to the time of the proton-transfer rate, the probability $P(t)$ that the excited state has not decayed by time t after excitation is given by

$$P(t) = \exp\left(\frac{-t}{\tau_f}\right)\int_0^\infty p(x) \exp[-k(x)t]\, dx \tag{14}$$

The first exponential accounts for the homogeneous radiative decay process, whereas the integral of the second exponential represents the inhomogeneous proton-transfer rate that depends on the cluster size. The observed transient fluorescence signal, $I(t)$, is a convolution of the instrument response function (IRF), $I_0(t)$, with the theoretical decay function

$$I(t) = Z_0\int_{-\infty}^{t} P(t - t')\, I_0(t')\, dt' \tag{15}$$

where Z_0 is a normalization constant for $I_0(t)$.

Finally, we derive an expression for the absolute fluorescence QY of the ROH. It is defined as the fraction of excited molecules which decay radiatively, by the emission of a photon. Because the latter is a unimolecular process, its transient rate is given by $\tau_f^{-1}P(t)$. The absolute QY is the time integral of this rate

$$\mathrm{QY} \equiv \int_0^\infty \tau_f^{-1} P(t)\, dt = \langle\tau\rangle/\tau_f \tag{16}$$

The second equality suggests that QY can also be interpreted as the ratio of the average excited-state lifetime, $\langle\tau\rangle \equiv \int_0^\infty P(t)\, dt$, and the radiative one.

Figure 5a shows the time-resolved emission of the ROH form of HPTS in ethanol and in an aqueous solution containing 3.45 M $MgCl_2$. In the ethanol solution, proton transfer from HPTS is ineffective within the limits of the excited-state lifetime. Therefore, the decay of ROH in ethanol is almost a single exponential with a lifetime of about 4.6 ns. In contrast to the exponential decay of HPTS in ethanol, the decay of the ROH in 3.45 M $MgCl_2$ is nonexponential at all times. The proton geminate recombination is small due to the effective screening of the Coulomb potential. We propose that the nonexponential decay arises from the inhomogeneity of the water structure in close proximity to the HPTS molecule in the presence of large salt concentrations. Figure 5b shows the time-resolved emission of the ROH of HPTS in a 3.3 M $MgCl_2$ solution along with the best fits of the geminate recombination model and the water cluster model. As seen in the figure, the fit of the water cluster model (the solid line) is excellent for more than 2 orders of magnitude. The geminate recombination model fails to fit the experimental decay at short and long times.

Parts c and d of Figure 5c,d show the fit of the cluster model to the time-resolved emission of the ROH band of HPTS in NaCl and $MgCl_2$, respectively. The fit of the model is rather good for short times, for both the low and high salt concentrations. It fails in fitting the long-time tail at low concentrations

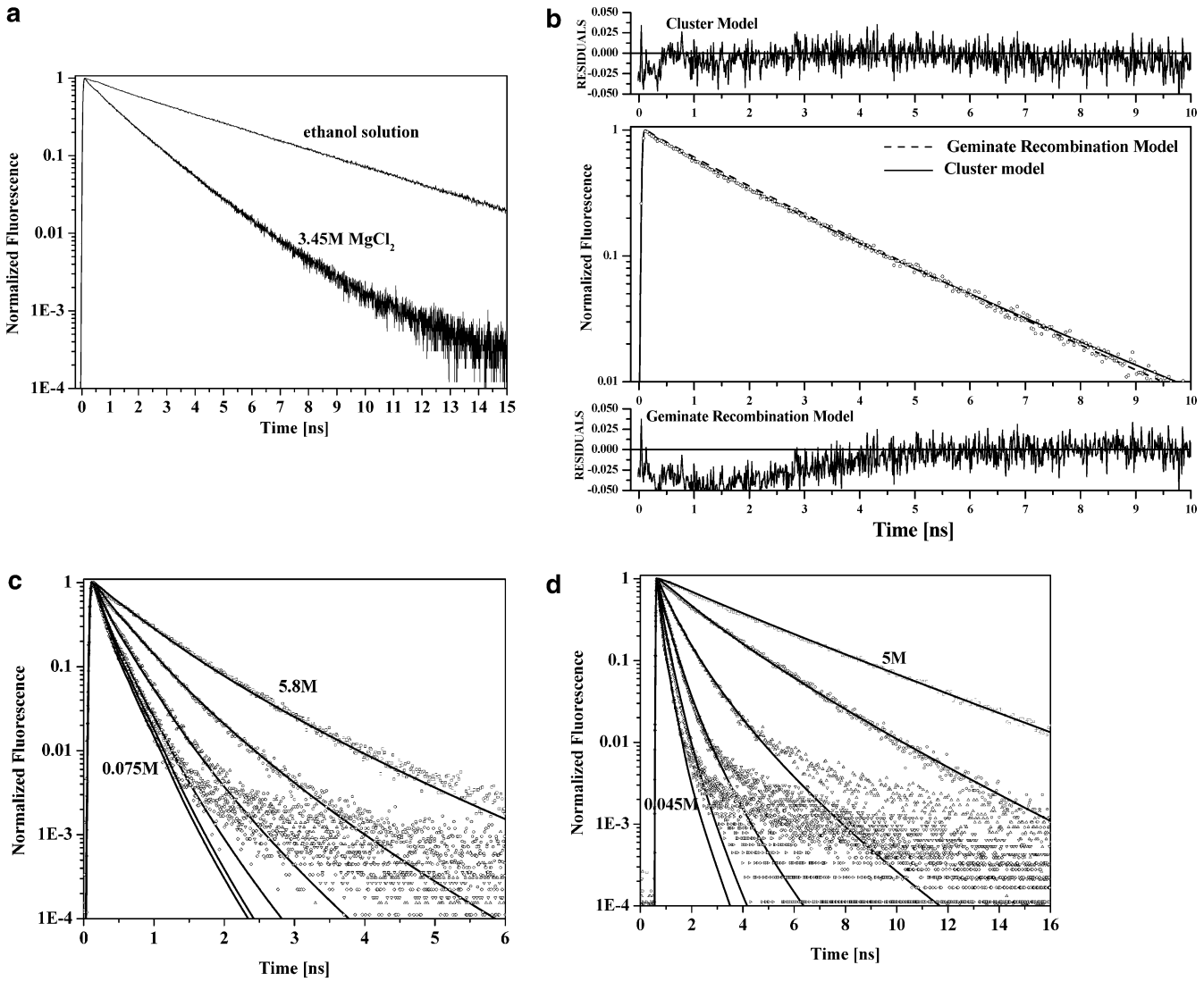

Figure 5. (a) Time-resolved emission of the ROH form of HPTS in neat ethanol and in an aqueous solution containing 3.45 M $MgCl_2$. Note the nonexponential decay of HPTS in $MgCl_2$. (b) Time-resolved emission of the ROH of HPTS in a 3.3 M $MgCl_2$ solution along with the best fits of the geminate recombination model (broken line) and the water cluster model (solid line). Note the good fit of the cluster model. (c) Fit of the cluster model (solid line) to the time-resolved emission (circles) of the ROH band of HPTS in NaCl, for several salt concentrations. (d) As for (c) but the salt is $MgCl_2$.

but fits much better the long time of high salt concentrations. The fitting parameters of the cluster model are A, the preexponential in the rate constant expression (see eq 13), the width of the clusters distribution, $2\sigma^2$, and the position of the Gaussian population, x_0, which is inversely proportional to the average cluster size (see eq 12). We set the preexponential value to be 1.5×10^{10} s^{-1} (independent of the salt concentration), slightly larger than the actual proton-transfer rate constant of HPTS in neat water 0.93×10^{10} s^{-1}. The values of the adjustable fitting parameters $2\sigma^2$ and x_0 are given in Tables 3 and 4 for NaCl and $MgCl_2$ solutions, respectively. The peak position of the Gaussian population, x_0, is almost fixed for low salt concentrations.

This finding is in accord with an almost independent proton-transfer and recombination rate constants at low salt concentrations. From the fitting procedure of the time-resolved emission by the geminate recombination model in NaCl solutions, the proton-transfer rate constant, k_d, is almost fixed up to about 1 M. The geminate recombination rate constant, k_r, is also fixed. For low salt concentrations, the time-resolved luminescence shape of both the ROH and RO^- bands is nearly independent of the salt concentration, because the screening of the Coulomb potential by the salt is almost complete. The screening effect is almost independent of the salt concentration at $c > 0.1$ M. In NaCl solutions of large concentration $c > 2$ M, the proton-transfer rate constant decreases and the shape of the ROH decay at early times deviates from exponential. In a large salt concentration, the cluster model fitting parameters x_0 and $2\sigma^2$ change with salt concentration. From the model, the larger the salt concentration the smaller the size of the average water cluster (large x_0) and the larger the width of its distribution (larger $2\sigma^2$).

TABLE 3: Kinetic Parameters for the Proton-Transfer Reaction of HPTS in H_2O/NaCl Using the Cluster Model[a,b]

C, [M]	$2\sigma^2$ (width)	x_0 (position)
0.290	0.25	0.00
0.580	0.25	0.00
0.970	0.25	0.20
1.45	0.25	0.35
2.32	0.33	0.52
2.58	0.37	0.60
3.31	0.40	0.85
4.64	0.44	1.48
5.8	0.48	2.10

[a] The preexponential factor $A = 15$ ns^{-1}. [b] The error in estimation of x_0 and $2\sigma^2$ is $\pm 15\%$.

TABLE 4: Kinetic Parameters for the Proton-Transfer Reaction of HPTS in $H_2O/MgCl_2$ Using the Cluster Model[a,b]

C, [M]	$2\sigma^2$ (width)	x_0 (position)
0.225	0.28	0.00
0.450	0.40	0.00
0.833	0.54	0.38
1.00	0.60	0.60
1.66	0.71	0.95
2.00	0.77	1.60
2.20	0.80	1.90
2.50	0.80	2.25
2.86	0.86	2.80
3.45	1.00	3.40
4.00	2.00	4.25
5.00	2.00	5.00

[a] The preexponential factor $A = 15$ ns^{-1}. [b] The error in estimation of x_0 and $2\sigma^2$ is ±15%.

In an $MgCl_2$ solution the effect of salt concentration on the decay profiles of the time-resolved emission is larger than that in NaCl. The value of the proton-transfer rate constant strongly decreases with salt concentration for concentrations larger than $c \geq 0.8$ M. The fitting parameters of the water cluster model drastically changes with the $MgCl_2$ concentration. The cluster size parameter, x_0, increases with the salt concentration. This is accompanied by an increase of the width of the population distribution. The average proton-transfer rate constant, according to the model, is given by $\bar{k} = A \exp(-x_0)$. For 5 M $MgCl_2$, $x_0 \approx 5$ we get $\bar{k} = 10^8$ s^{-1}. This value is 0.01 of the rate constant in neat water or at low salt concentration and is smaller by a factor of 2 than the radiative rate of ROH. The Gaussian width increases by a factor of 6 from $2\sigma^2 = 0.3$ at low salt concentrations to about 2 at high salt concentrations.

Steady-State Emission. Parts a and b of Figure 1a,b show the steady-state emission of HPTS in the presence of NaCl and $MgCl_2$ salts in aqueous solutions. The larger the salt concentration, the larger the ROH band emission intensity and the lower the RO^- intensity. As shown in Figures 2−4 and the analysis of the time-resolved emission using the geminate recombination model, the proton-transfer rate slows with the increase in salt concentration. An additional enhancement of the salt effect on the steady-state emission of HPTS arises from the large increase in the proton recombination (see eq 5) due to the increase of the ratio k_r/k_d and the decrease in the proton diffusion constant with salt concentration. The recombination rate constant slightly increases with salt concentration k_r whereas the proton-transfer rate constant k_d strongly decreases. The overall salt effect is a large increase in the amplitude of the geminate recombination long-time fluorescence tail of ROH, which amounts to the coalescence of the initial decay (the proton transfer) with the fluorescence tail arising from the reversible proton recombination. The net result is that the proton-transfer quantum yield drops with the salt concentration increase and at about 5 M $MgCl_2$ the proton is not really transferred to the solvent.

Integrating the time-resolved emission of the ROH band measured at 435 nm provides the average lifetime of the ROH. Figure 6 shows the relative intensity of the ROH band taken from the steady-state emission spectrum shown in Figure 1b (circles) (normalized to the ROH intensity of 5 M) and the time-integrated average lifetime (normalized to the steady-state intensity of 5 M $MgCl_2$ as a function of the $MgCl_2$ concentration). As seen in the figure the time-integration values of the ROH* population fits the normalized steady-state intensity of the ROH band nicely. The time integration of the time-resolved emission computer fit of both models (eqs 6 and 16) gives also an excellent match to the steady-state data.

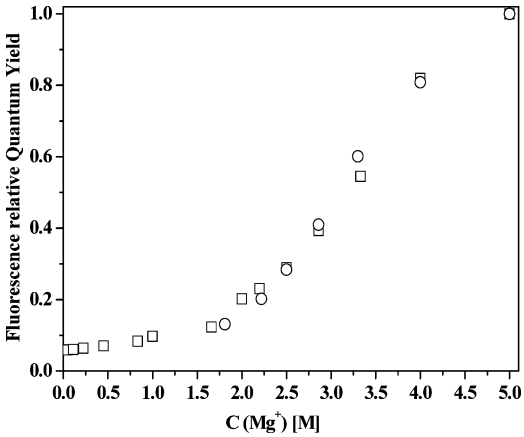

Figure 6. Relative intensity of the ROH emission band taken from the steady-state emission spectrum shown in Figure 1b (circles) and the time-integrated average lifetime (squares, calculated from the time-resolved emission) as a function of the $MgCl_2$ concentration (squares).

ROH Long-Time Fluorescence Tail. Figure 7a shows on a log−log plot the time-resolved emission of ROH in water, 0.05 M NaCl and 0.045 M $MgCl_2$. The experimental data are multiplied by $\exp[t/\tau_f]$ to account for the finite excited-state lifetime. According to the long-time asymptotic expression given by eq 5 of the geminate recombination model, the decay should be a power law of $t^{-3/2}$ for a three-dimensional diffusion space. The $t^{-3/2}$ asymptotic law is reached only when a quasi-equilibrium is established between the proton distribution $p(r,t)$- and the ROH population. The time lag needed for establishing a quasi-equilibrium depends on three parameters k_d, k_r and D. The larger these parameters, the shorter the time lag. At times shorter than this time lag, the ROH emission decays nearly exponentially. The slope of an exponential decay on a log−log scale is not constant but depends on time. Figure 7a also shows such an exponential decay with a time constant of 100 ps, the value of $1/k_d$ of HPTS in neat water. For the ROH emission, the geminate recombination model predicts that the slope of $t^{-3/2}$ should be maintained for all salt concentrations, but the amplitude of the long-time tail should decrease because of the Coulomb potential screening by the solution as the salt concentration increases. At small concentrations of $MgCl_2$ salt, $c = 0.045$ M the measured slope shown in Figure 7a as a dashed line at short times (between 0.3 and 2 ns) is −2.5, much larger than the predicted slope of $t^{-3/2}$. Careful examination of the simulations shown as a solid line in Figure 2 shows that at times prior to the condition of the quasi-equibrium (the power law of $t^{-3/2}$), the slope of the signal on a log−log plot has indeed a decent steeper than $t^{-3/2}$.

For high salt concentrations, we find that all the parameters that determine the amplitude of the long-time tail change with the salt concentration. Figure 7b shows the time-resolved emission of ROH on a log−log scale of ROH in the presence of large concentrations ($c \geq 0.97$ M) of NaCl. The long-time slopes of the ROH decay are larger than −3/2. At the highest concentrations, the condition of reaching the $t^{-3/2}$ power law is shifted to longer times, $t > 10$ ns. Also, the relative amplitude of the long-time asymptotic tail drops by more than an order of magnitude at about 2.8 M of NaCl. Figure 7c shows a computer simulation on a log−log scale of the geminate recombination model with the parameters used to fit the decay of several solutions of NaCl. As seen from the figure, the $t^{-3/2}$ slope is reached only after very long times. In a real ESPT experiment the excited-state population of ROH decays via two channels: the reactive channel to produce RO^- and the radiative decay

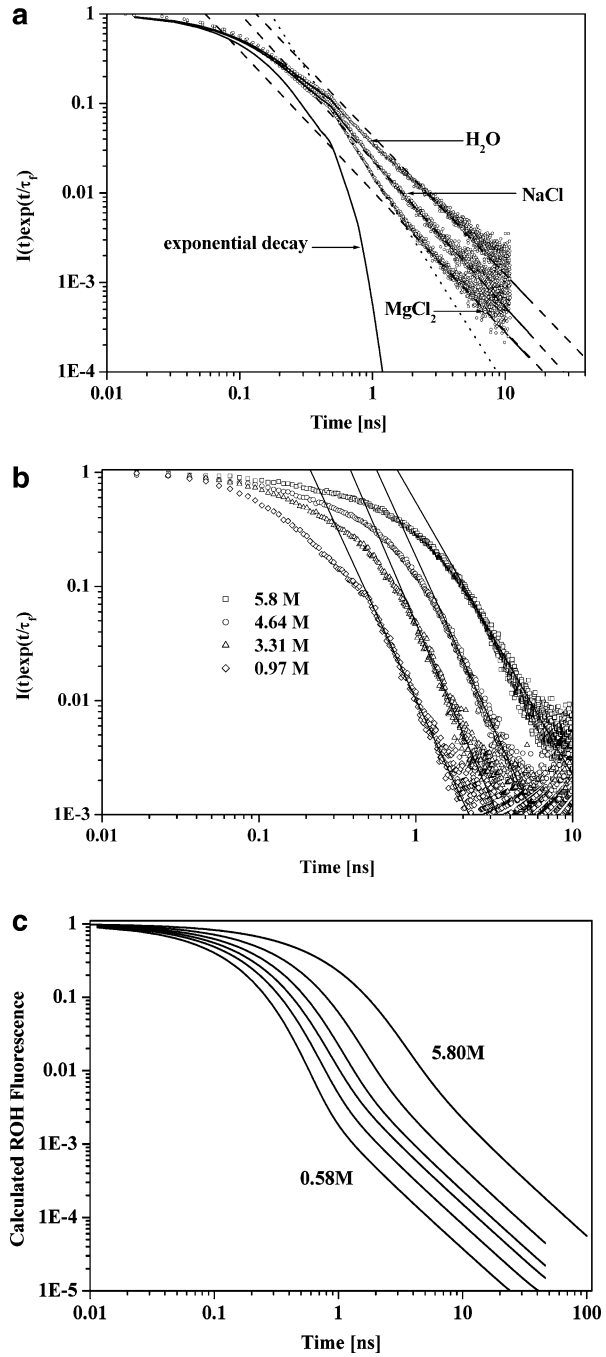

Figure 7. (a) log−log plot of the time-resolved emission of ROH in water, 0.05 M NaCl and 0.045 M $MgCl_2$ (circles) along with a computer fit to the geminate recombination model (solid line). The experimental data are multiplied by $\exp[t/\tau_f]$ to account for the finite excited-state lifetime. (b) log−log plot of the time-resolved emission of ROH at various salt concentrations of NaCl multiplied by $\exp[t/\tau_f]$ to account for the finite excited-state lifetime. (c) Computer simulation of the time-resolved emission of ROH on a log−log scale using the geminate recombination model with the parameters used to fit the experimental results of several solutions of NaCl.

repopulating the ground state, $\tau_f \approx 5$ ns. Thus, the ROH emission signal decays with an additional exponential rate $\exp[-t/\tau_f]$, which limits the time window for observing the $t^{-3/2}$ power law to rather short times of about twice the excited-state lifetime, i.e., about 10 ns. At 20 ns (4 lifetimes), the signal intensity drops by a factor of $e^{+4} = 55$ and the signal-to-noise ratio, S/N, by $\sqrt{55}$. Thus, for slow proton-transfer rates and a slow diffusion constant, the power law condition is beyond the reach of the experimental conditions.

The situation in an $MgCl_2$ solution is even worse. The large drop in k_d for high salt concentrations shifts the semi-equilibrium condition to a later time than the same concentration of salt in NaCl solutions. In 1 M solutions of $MgCl_2$, the slope between 0.4 ns and about 2 ns is −2.5. From the simulation using the SSDP program, we find that the conditions for the asymptotic power law $t^{-3/2}$ are reached beyond 4 ns. As previously mentioned, the time-dependent excited state ROH population drops exponentially with time due to the radiative process, and hence, at such long times, it is impractical to get a decent signal and determine the actual slope.

Summary

We studied the excited-state proton transfer and the geminate recombination process in HPTS in water in the presence of two electrolytes, NaCl and $MgCl_2$. We used the time-correlated single photon counting technique to measure the time-resolved emission of both the protonated ROH* and deprotonated RO^{-}* forms of the photoacid. We found that for low salt concentrations, we can use the geminate recombination model to quantitatively account for the photoprotolytic process using the Coulomb screened potential. As the salt concentration increases, the screened Coulomb attraction decreases and thus the proton geminate recombination process is less effective.

At higher salt concentrations the proton-transfer rate constant decreases while the recombination rate constant slightly increases. For a saturated solution of $MgCl_2$ (about 5 M at room temperature), the proton-transfer rate constant is smaller by a factor of 100 than that of pure water. The steady-state emission consists of only a single band: that of the protonated photoacid. For excited-state proton transfer in this large concentration range of $MgCl_2$, we were able to get a good fit of the experimental data with a model based on the distribution of proton-transfer rates. The model is consistent with inhomogeneous water clusters surrounding the HPTS molecules in concentrated solutions. In pure water, a proton is transferred to a water cluster of a size about ≥10 water molecules. [19,20,31] In a concentrated solution, such a large number of free water molecules is not available because an Mg^{2+} ion binds about 14 water molecules.[31]

Acknowledgment. We Thank Prof. N. Agmon for his helpful and fruitful suggestions and discussions. This work was supported by grants from the Binational US−Israel Science Foundation, the U.S. National Foundation and the James-Franck German-Israel Program in Laser-Matter Interaction.

References and Notes

(1) Bell, R. P. *The Proton in Chemistry*, 2nd ed.; Chapman and Hall: London, 1973.
(2) *Proton-Transfer Reaction*; Caldin E. F., Gold V., Eds.; Chapman and Hall: London, 1975.
(3) (a) Weller, A. *Prog. React. Kinet.*, **1961**, 1, 189. (b) *Z. Phys. Chem. N. F.* **1958**, *17*, 224.
(4) (a) Eigen, M. *Angew. Chem.*, Int. Ed. **1964**, 3, 1. (b) Eigen M.; Kruse W.; Maass G.; De Maeyer, L. *Prog. React. Kinet.* **1964**, *2*, 285.
(5) Ireland, J. E.; Wyatt, P. A. *Adv. Phys. Org. Chem.* **1976,** *12*, 131.
(6) (a) Gutman, M.; Nachliel, E. *Biochim. Biophys. Acta* **1990**, *391*, 1015. (b) Pines, E.; Huppert, D. *J. Phys. Chem.* **1983**, *87*, 4471.
(7) Kosower, E. M.; Huppert, D. *Annu. Rev. Phys. Chem.* **1986**, *37*, 127.
(8) Tolbert, L. M.; Solntsev, K. M. *Acc. Chem. Res.* **2002**, *35*, 1.
(9) Rini, M.; Magnes, B. Z.; Pines, E.; Nibbering, T. J. *Science* **2003**, *301*, 349.
(10) Prayer, C.; Gustavsson, T.; Tarn-Thi, T. H. *Fast Elementary Processes in Chemical and Biological Systems*; 54th International Meeting of Physical Chemistry; AIP: NY, 1996; p 333.
(11) Tran-Thi, T. H., Gustavsson T., Prayer, C., Pommeret S., Hynes J. T. *Chem. Phys. Lett.* **2000**, *329*, 421.
(12) Agmon, N. *J. Phys. Chem. A* **2005**, *109*, 13.

(13) Smith, K. K.; Huppert, D.; Gutman, M.; Kaufmann, K. *Chem. Phys. Lett*. **1979**, *64*, 22.
(14) Clark, J. H.; Shapiro, S. L.; Campillo, A. J.; Winn, K. J. *J. Am Chem. Soc*. **1979**, *101*, 746.
(15) Politi, M. J.; Fendler, J. H. *J. Am. Chem. Soc*. **1984**, *106*, 265.
(16) Pines, E.; Huppert, D. *J. Chem. Phys*. **1986**, *84*, 3576.
(17) Pines, E.; Huppert, D.; Agmon, N. *J. Chem. Phys*. **1988**, *88*, 5620.
(18) Agmon, N.; Goldberg, S. Y.; Huppert, D. *J. Mol. Liq.* **1995**, *64*, 161.
(19) Huppert, D.; Kolodney, E.; Gutman, M.; Nachliel, E. *J. Am. Chem. Soc.* **1982**, *104*, 6949.
(20) Kebarle, P. In *Thermochemical Information from Gas-Phase Ion Equilibria*; Ausloos, P., Ed.; Plenum Press: New York, 1975; NATO Adv. Study Inst., Ser. B, p 6.
(21) Robinson, R. A.; Stokes R. H. *Electrolyte Solutions*, 2nd ed.; Butterworth: London, 1959; Appendices 1.1 and 6.2.
(22) Rice, S. A. In *Diffusion-Limited Reactions*; Computers and Chemical Kinetics, Vol. 25; Bamford, C. H., Tipper, C. F. H., Compton, R. G., Eds.; Elsevier: Amsterdam, 1985.
(23) Agmon, N. *J. Chem. Phys.* **1984**, *81*, 2811.
(24) Pines, E.; Huppert, D.; Agmon, N. *J. Phys. Chem.* **1991**, *95*, 666.
(25) Krissinel, E. B.; Agmon, N. *J. Comput. Chem* **1996**, *17*, 1085.
(26) Lewis, G. N.; Doody, T. C. *J. Am. Chem. Soc*. **1933**, *55*, 3504.
(27) Haar, H. P.; Klein U. K. A.;. Hfiner, F. W.; Hauser M. *Chem. Phys. Lett*. **1977**, *49*, 416.
(28) Searcy, J. Q.; Fenn, J. B. *J. Chem. Phys.* **1974**, *61*, 5282.
(29) Kraemer, W. P.; Diercksen, G. H. F. *Chem. Phys*. *Lett.* **1970**, *5*, 463.
(30) Newton, M. D.; Ehrenson, S. *J. Am. Chem. Soc.* **1971**, *93*, 4971.
(31) Hasted, J. B.; Ritson, D. M.; Collie, C. H. *J. Chem. Phys.* **1948**, *16*, 1.
(32) Pines, E.; Fleming, G. R. *Chem. Phys. Lett.* **1994**, *183*, 393.
(33) Eigen, M.; Tamm, K. *Z. Elektrochem.* **1962**, *66*, 93, 107.
(34) Knochenmuss, R.; Fischer, I.; Lührs, D.; Lin, Q. *Isr. J. Chem*. **1999**, *39*, 221.
(35) Gepshtein, R.; Huppert, D.; Agmon, N. *J. Phys. Chem*. *A* **2006**, *110*, 4434.